Anti-icing Skin with Micro-nano Structure Inspired by Fargesia Qinlingensis

YAN Zexiang[1,2], *HE Yang*[1,2*], *YUAN Weizheng*[1,2*]

1. Key Lab of Micro/Nano Systems for Aerospace, Ministry of Education, Northwestern Polytechnical University, Xi'an 710072, P. R. China;

2. Shaan'xi Key Lab of MEMS/NEMS, Northwestern Polytechnical University, Xi'an 710072, P. R. China

(Received 8 March 2023; revised 8 April 2023; accepted 24 April 2023)

Abstract: Aircraft icing has a significant impact on flight safety, as ice accumulation on airfoils and engines can cause aircraft stalls. Developing anti-icing technology that can adapt to harsh and cold environment presents a challenge. Here, we propose a new anti-icing skin with micro-nano structure inspired by the bamboo leaf called Fargesia qinlingensis. A multilayer non-uniform height (MNH) micro-nano structure is proposed based on the Fargesia qinlingensis surface structure. The anti-icing mechanism of the MNH micro-nano structure is revealed. The flexible large-area MNH micro-nano structure is fabricated based on hierarchical assembly method. Compared with the smooth surface, the ice adhesion strength of the prepared bio-inspired surface is reduced by 80%, indicating that the MNH micro-nano structure inspired by Fargesia qinlingensis has ice-phobic effect. Based on this, an anti-icing hybrid skin based on bionics and electric heating is developed. The anti-icing hybrid skin has successfully completed the anti-icing function flight test on the UAV. To realize the effective anti-icing function under super cold conditions, the anti-icing hybrid skin has been applied on a certain type of UAVs. The bio-inspired anti-icing skin has broad application prospects in large transport aircraft, helicopters, wind power generation, and high-speed trains.

Key words: aircraft anti-icing; bio-mimic surface; micro-nano structure; functional aircraft skin

CLC number: V244.15 **Document code:** A **Article ID:** 1005-1120(2023)02-0115-09

0 Introduction

Aircraft icing has great impact on the flight safety, and the anti-icing technology for aircraft in harsh and cold environment is a challenge[1-2]. According to the International Civil Aviation Organization's "2020—2022 Global Aviation Safety Plan", aircraft icing is still one of the important issues for the global aviation industry. However, the existing anti-icing technologies for aircraft such as liquid, pneumatic, gas-thermal, and electric-thermal methods[3-6] generally have the problems of large load and high energy consumption, so they cannot be used for aircraft with small load and low power, such as unmanned aerial vehicles (UAVs)[7-8].

The biomimetic micro-nano structure surface provides a promising direction for anti-icing research[9]. Since Barthlott et al.[10] proposed the "lotus effect" in 1997, the anti-icing effect achieved by the superhydrophobic surface has become a popular research topic[11]. Superhydrophobicity generally refers to a surface where the three-phase contact angle is greater than 150°, and the contact angle hysteresis is less than 10°. The water droplets on the superhydrophobic surface are likely to bounce, which greatly shortens the solid-liquid contact time. Moreover, because the superhydrophobic surface is usually a regular array structure, it reduces the probability of ice nucleation and increases the delay time of ice formation[12]. Furthermore, researchers proposed anti-icing surfaces inspired by various animals and plants[13], such as rose petals[14], butterfly

*Corresponding authors, E-mail addresses: heyang@nwpu.edu.cn; Yuanwz@nwpu.edu.cn.

How to cite this article: YAN Zexiang, HE Yang, YUAN Weizheng, et al. Anti-icing skin with micro-nano structure inspired by fargesia qinlingensis[J]. Transactions of Nanjing University of Aeronautics and Astronautics, 2023, 40(2): 115-123.

http://dx.doi.org/10.16356/j.1005-1120.2023.02.001

wings[15], rice leaves[16]. These studies are all based on the superhydrophobic phenomenon of living organisms in nature, imitating their microstructure, and preparing the anti-icing surfaces through photolithography, mechanical processing, electrochemical deposition, femtosecond laser processing and other methods[17-21]. However, recent studies have pointed out the shortcomings of superhydrophobic surfaces in outdoor environments[22-23]. Under the impact of outdoor rainwater, wind load, etc., some tiny water droplets will infiltrate the surface microstructure, which will reduce the superhydrophobic performance and eventually lead to the failure of anti-icing.

Many unique phenomena in nature are the results of thousands of years of evolution to adapt to the environment. Although the bionic superhydrophobic surface has the anti-icing effect, these plants are not in direct contact with ice and snow after all. We find that there is a unique plant in Qinling Mountains — Fargesia qinlingensis, which has a surface that is not easily adhered to ice and snow, as shown in Fig.1. As the climate boundary, since 1980 — 2016, there have been 114 regional alpine snow events in Qinling Mountains with an average time of 16 d each time. As an evergreen plant, Fargesia qinlingensis can keep its leaves basically free of ice and snow in Qinling Mountains at an altitude of 1 500 m, showing excellent anti-icing effect.

(a) Fargesia qinlingensis leaves under ice and snow environment in Qinling Mountains (b) Anti-icing effect between Fargesia qinlingensis and lotus leaves

Fig.1 Anti-icing performance of Fargesia qinlingensis leaves

A multilayer non-uniform height (MNH) micro-nano structure is proposed based on the Fargesia qinlingensis surface structure. The anti-icing mechanism of the MNH micro-nano structure is elucidated, and a fabrication method based on hierarchical assembly is provided for preparing flexible, large-area MNH micro-nano structures. An anti-icing skin based on bionics and electric heating is developed. The anti-icing skin has successfully completed the anti-icing function flight test on small-to-medium-sized UAVs, and it has been applied on a certain type of UAVs.

1 Anti-icing Mechanism of Fargesia Qinlingensis

The surface structure and chemicals of the Fargesia qinlingensis leaves are analyzed. The leaves are from the watershed at Fengyu valley in Qinling Mountains. Plants in good growth condition are selected, and 5 leaves with the length of no less than 4 cm are selected from each plant. Leaf samples are washed with ethanol immediately after harvest, and sealed in test tubes filled with deionized water. The time from harvest to experiment is less than 6 h to ensure freshness. Scanning electron microscopy (VEGA3, SBH, TESCAN Company Ltd) is used to observe the morphology of leaf samples, and the results are shown in Fig.2. The leaf surface of Fargesia qinlingensis has a multilayer structure with the scale covering a range from 100 μm to 100 nm. Its multiscale structure is composed of four layers: The first layer is columnar structures arranged with regular spacing, with a height of about 50 μm; the second layer is a drop-like structure arranged along the leaf growth direction, with a height of 20 μm and

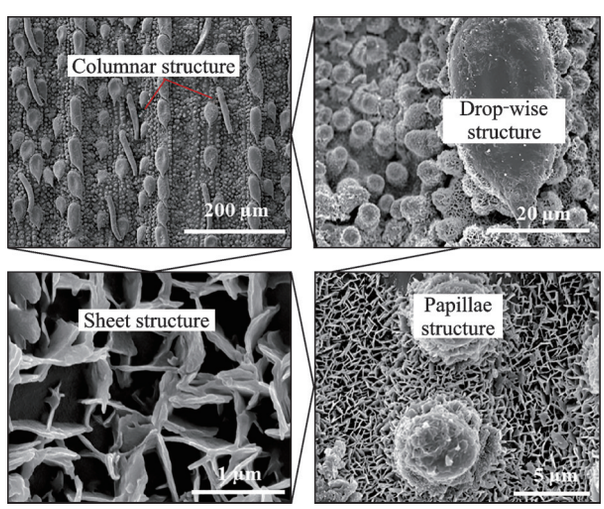

Fig.2 SEM images of MNH micro-nano structure of Fargesia qinlingensis

spacing of 100 μm; the third layer is composed of densely arranged papillae structures with a diameter of 5 μm; the fourth layer is nanoscale three-dimensional sheet structure.

The unique MNH micro-nano structure of Fargesia qinlingensis is the key to its ability to repel ice. For common regular array microstructures, supercooled microscopic water droplets will infiltrate into the gaps of the structure, which will weaken the superhydrophobicity and lead to surface icing. At the same time, the ice embedded in the structure will also produce the mechanical interlocking, increasing the ice adhesion strength. However, the MNH micro-nano structure of Fargesia qinlingensis is conducive to the bouncing of supercooled water droplets, and enhances the anti-wetting ability. Even if some water droplets fail to leave the surface in time and freeze eventually because of the high liquid water content and strong airflow, the ice adhesion strength is relatively low. This is because the multilayer and multiscale micro-nano structure forms more cavities, and the ice on top is more likely to generate local stress concentration. Therefore, the ice-solid interface tends to produce micro-cracks, which effectively reduces the adhesion strength. The schematic diagram of anti-icing mechanism of Fargesia qinlingensis is shown in Fig.3.

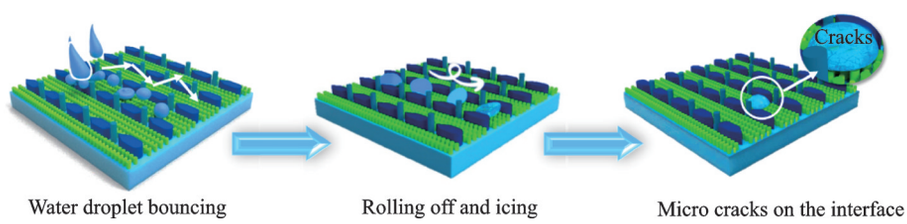

Fig.3 Schematic diagram of the anti-icing mechanism of Fargesia qinlingensis

2 Fabrication of Anti-icing Skin Inspired by Fargesia Qinlingensis

The fabrication of large-scale and complex topographical structures has always been a challenge for micro-nano processing technology. The topography of Fargesia qinlingensis involves structures at different scales. Using a single mask etching method cannot produce multilayer micro-nano structures, and adding masks to achieve structures with different heights is also difficult. Here, we propose a fabrication method based on hierarchical assembly to realize a flexible large-area MNH micro-nano structure. First, large-area single-layer structure surfaces are prepared. Then, the layers are combined by adjusting the interfacial adhesion force, and a large-area flexible multi-layer structure is obtained. The schematic diagram of the fabrication process for the MNH micro-nano structure is shown in Fig.4.

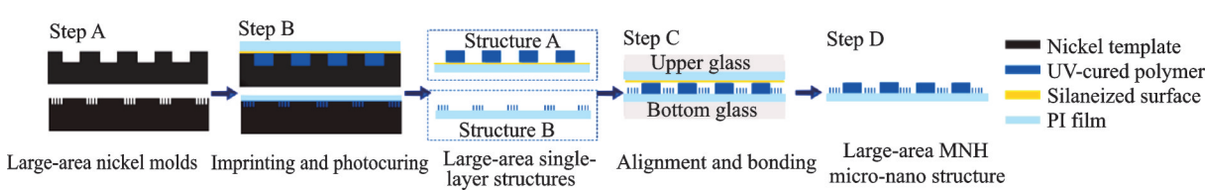

Fig.4 Fabrication process of MNH micro-nano structures

Patterned photoresist structures on the nickel substrate are obtained through photolithography, and then the nickel mold master with fine microstructure is obtained through electroforming. Multiple nickel molds of the same size are obtained by secondary electroforming. An aligner is used to realize the preparation of large-area negative templates (Step A). Furthermore, large-area single-layer microstructures are obtained on the polyimide substrate by imprinting and photocuring (Step B). Here, the drop-like structure (Structure A) is fabricated differently from the papillae structure (Struc-

ture B). More specifically, for the drop-like structure, a pre-prepared smooth and thin ultraviolet-cured polymer (UV-cured polymer) is placed in 1H, 1H, 2H, 2H-perfluorooctyltriethoxysilane solution for 2 h, and is dried in the oven with 60 ℃, 30 min. The adhesion of the silaneized surface is reduced due to the formation of CF^3 groups. The silanized UV polymer, used as a transfer layer, is covered on the nickel template that has been coated with UV-cured prepolymer, and is irradiated with the UV curing machine for 10 s with the irradiation energy of 12 950 mJ/cm^2. Then Structure A is obtained after the UV-cured polymer is peeled off. For the papillae structure, UV-cured polymer is applied to the nickel template and covered with a PI film. Structure B is also fabricated after photocuring and peeling. Referring to the wafer bonder, a set of multilayer microstructure alignment device is designed. The single-layer Structure A is attached upside down to the upper glass platform. The image of Structure A is transferred to a display screen by a charge-coupled device, and calibration lines are drawn along the feature edges of Structure A on the screen. Structure B is placed on the lower platform, with the three-axis turntable and microscope, the alignment of the multi-layer structure is realized by adjusting Structure B according to the calibration line. The aligned structure is treated by corona discharge for 1 min, so that the structural layers are fully bonded (Step C). Since the adhesion force between the interface of Structures A and B is greater than that between the interface of the transfer layer and Structure A, Structure A can be successfully peeled off and the large-area MNH micro-nano structure is finally obtained (Step D).

The SEM image of the simplified structure inspired by Fargesia qinlingensis is shown in Fig. 5. The MNH micro-nano structure has a staggered arrangement of drop-like and papillae structures, in which the length of the drop-liked structure is 45 μm, the width is 20 μm, the height is 20 μm, and the lateral spacing is 50 μm. The papillae structure is 5 μm in diameter and 5 μm in height. The static contact angle of the surface is 140.9°, and the sliding angle

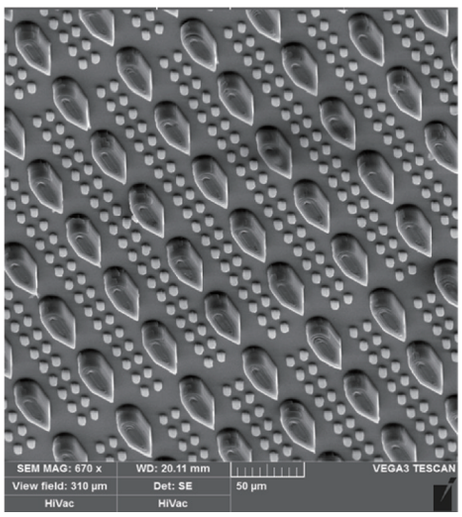

Fig.5 SEM image of the prepared MNH micro-nano structure

is 10.2°, demonstrating a fine hydrophobic property.

The ice adhesion strength of the prepared MNH micro-nano structure is measured by a self-made adhesion force measuring equipment with the ambient temperature −10 ℃, and the water droplet is 15 μL. After the water drop freezing on the surface, the force probe is driven by the motor to remove the ice, and the force curve is recorded. According to the image method, the contact area between the ice drop and the surface is obtained, and the ice adhesion strength is calculated. Fig.6 shows the results of ice adhesion strength of the MNH micro-nano structure and the smooth surface. The results indicate that the MNH micro-nano structure reduces the ice adhesion strength by 80% compared with the smooth surface.

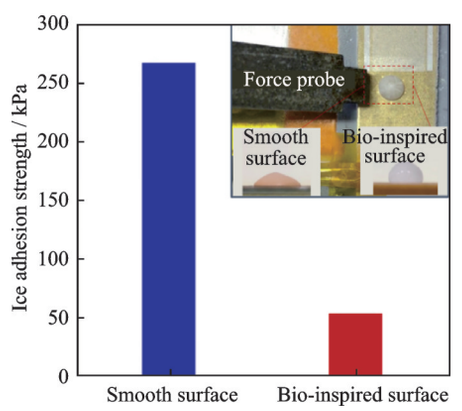

Fig.6 Results of ice adhesion strength of MNH micro-nano structure and smooth surface

3 Ice Wind Tunnel Test of Anti-icing Skin

Previous research has proved that under the impact of high-speed cold airflow, it is difficult to achieve long-term and efficient anti-icing effect only by passive anti-icing technology. The consensus is that a combination of active and passive anti-icing technologies is currently the most reliable solution to aircraft icing problems. Therefore, we propose an anti-icing scheme, adding a surface insulation layer, a metal heating layer and a bottom insulation layer under the bionic anti-icing structure layer to obtain an anti-icing hybrid skin. The bionic anti-icing structure layer can prevent the accumulation of supercooled water droplet, and the electric heating layer ensures the efficient anti-icing process in extremely harsh environments. The upper and lower insulation layers are both PI films. The metal heating layer is made from constantan and fabricated by photolithography and etching. Constantan has high resistivity and thermal conductivity (4.8×10^{-7} Ω·m and 118 W/m·K, respectively). At the same time, the good ductility and bending resistance of constantan guarantee the integrity when attaching to the airfoil.

When an aircraft passes through a supercooled cloud, the impact of supercooled water droplets in different areas of the airfoil is various. Adopting a single electrothermal power density cannot achieve a reasonable distribution of energy and may even cause shortage for aircraft energy supply. Therefore, it is necessary to perform chordwise power density partitioning on the electric heating of the skin to reduce anti-icing energy consumption and ensure a longer endurance time. A low energy consumption bionic anti-icing system based on power density partition is proposed. The numerical calculation method is used to analyze the anti-icing power density distribution regularity of the airfoil surface under specific working conditions, and the anti-icing hybrid skin is designed according to the calculated power density distribution.

Considering the actual flight requirements, the energy consumption requirements for the UAV anti-icing system are the most stringent among other aircraft. Here, a certain type of the UAV is selected as the experimental object for research. According to the flight altitude, speed, attack angle of the UAV, and the meteorological design standards under typical conditions in Appendix C of CCAR-25[24], the specific working conditions are determined as: wind speed 40 m/s, temperature −10 ℃, attack angle 2°, LWC 0.503 g/m^3, MVD 20 μm (LWC refers to the supercooled water content and MVD the average diameter of supercooled water droplets). In this experiment, an airfoil model scaled down by a factor of 0.5 is used, and the airfoil profile at approximately 7.7 m away from the aircraft centerline is extracted from the original wing as the scaled object. The coupled algorithm is used to calculate the external flow field of the airfoil, and the water droplet phase control equation is solved to obtain the local water droplet collection coefficient on the surface, as shown in Fig.7(a). The icing protection range determined by the droplet collection is S: −40—30 mm. S represents chordwise distance along the airfoil surface, with negative values indicating distance along the lower surface and positive values indicating distance along the upper surface. The theoretical anti-icing power density distribution regularity is obtained by calculating the anti-icing heat load in different areas of the airfoil.

Considering the anti-icing effect of the MNH micro-nano structure, the accumulation of water droplets is decreased, leading to the reduction of the heat flow related to water droplets. Therefore, the correction coefficient is used here to characterize the influence of the MNH micro-nano structure surface on the calculation of the anti-icing heat flow. Experiments on the capture rate of supercooled water droplets are carried out on the surface of MNH micro-nano structure in a low temperature environment. The experimental results show that under the working conditions mentioned above, the MNH micro-nano structure surface can reduce the water collection by about 90% compared with the ordinary surface. The corrected theoretical anti-icing thermal load is shown in Fig.7(b), in which the line is the calculated theoretical anti-icing power density distribution regularity and the histogram is the partition power

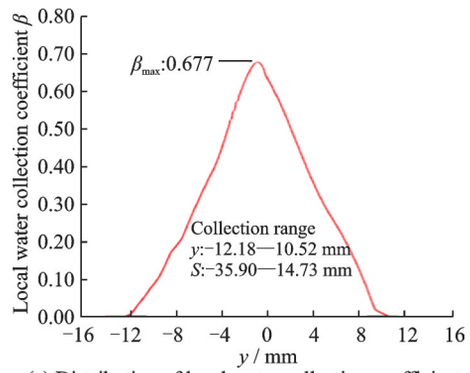

(a) Distribution of local water collection coefficient

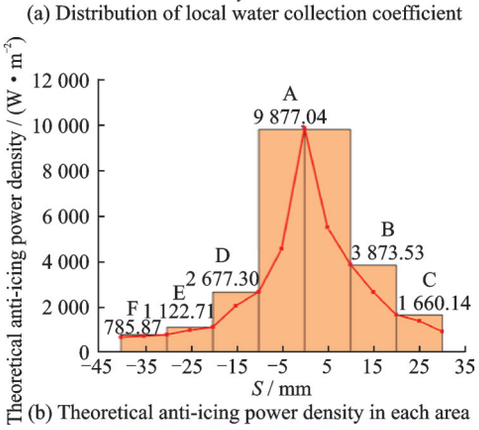

(b) Theoretical anti-icing power density in each area

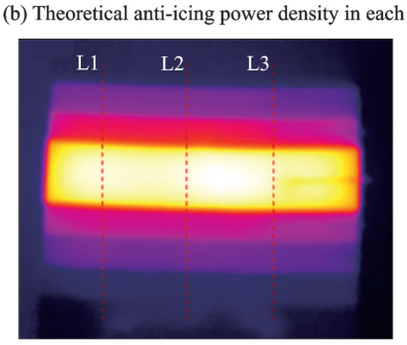

(c) Infrared image of heat distribution on the skin surface

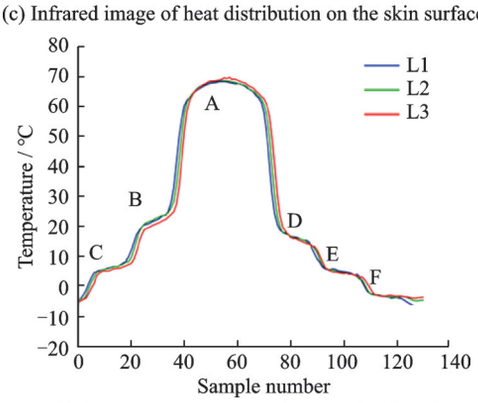

(d) Temperature curves at three marked locations

Fig.7 Design of anti-icing hybrid skin

density value (the maximum theoretical anti-icing thermal load in each area). A handheld thermal camera (Fluke, TiS60+, Shanghai, measurement accuracy within ±2 ℃ or within 2%, thermal sensitivity ≤0.045 ℃) is used to test the thermal distribution characteristics at −10 ℃, and the results reveal that the thermal distribution of the anti-icing hybrid skin has good uniformity under low temperature conditions, as shown in Figs. 7(c, d), where A—F represent different areas of airfoil and L1, L2, L3 the temperature test line selected in Fig.7(c).

The anti-icing performance of the anti-icing hybrid skin is verified in the ice wind tunnel. The anti-icing hybrid skin is attached to the surface of the airfoil, and the test conditions are shown in Table 1. The test results are displayed in Fig.8. There is no obvious icing on the leading edge and the upper and lower airfoil parts, which is obviously distinct from the part without the skin. Therefore, it is verified that the anti-icing hybrid skin has good anti-icing ice performance.

Table 1 Experimental conditions for anti-icing performance test of anti-icing skin

Wind speed/ (m • s^{-1})	Temperature/℃	MVD/ (g • m^{-3})	LWC/ (g • m^{-3})	Pressure/ MPa	Water pressure/ MPa
40	−10.1	18.3	0.503	0.15	0.1

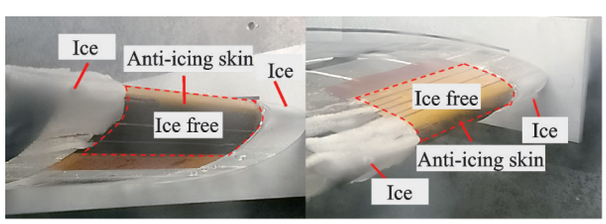

(a) The lower airfoil (b) The upper airfoil and leading edge

Fig.8 Ice wind tunnel test results for anti-icing hybrid skin

4 Applications

The flight test of the developed anti-icing hybrid skin demonstrates that the tested UAV successfully completes the flight mission at an altitude of 1—4 km, a maximum flight altitude of 8 km, a cruising speed of 40 m/s and a temperature of −10——3 ℃. At present, the anti-icing hybrid skin has been successfully applied on a certain type of UAVs, becoming the world's first mid-airway long-endurance UAV with anti-icing function. Fig. 9 is the photo of the flight test of the anti-icing hybrid skin. Moreover, the anti-icing skin inspired by Fargesia qinlingensis has broad application prospects in the fields of large transport aircraft, helicopters,

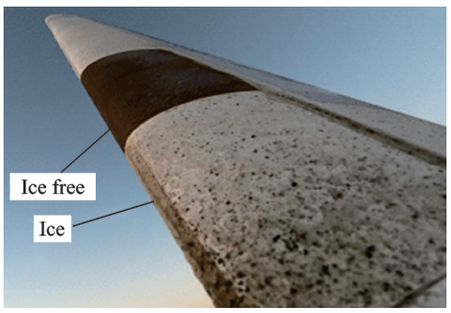

Fig.9 Photo of the flight test of the anti-icing hybrid skin

wind power generation, and high-speed trains.

5 Conclusions

Aircraft icing poses a great threat to flight safety, and the bionic micro-nano structured surface provides a new direction for anti-icing technology. A unique plant in Qinling Mountains with excellent anti-icing effect called Fargesia qinlingensis is found. The MNH micro-nano structure inspired by Fargesia qinlingensis is proposed, and the anti-icing mechanism of the multilayer structure is discussed. The multilayer and multiscale structure enhances the bouncing behavior of supercooled water droplets, and the large number of cavities reduce ice adhesion by facilitating formation of micro-cracks on the interface. A method for the preparation of flexible large-area micro-nano structures based on hierarchical assembly is proposed. The monolayer is fabricated through imprinting and photocuring, and surface modification by fluorosilanes and corona discharge is applied to realize the combination of the layers. The ice adhesion strength of the obtained anti-icing MNH micro-nano structure surface is reduced by 80%, comparing with the smooth surface. Considering the actual flight environment, a low energy consumption bionic anti-icing system based on power density partition is proposed. The UAV flight test demonstrates that the developed anti-icing hybrid skin has great anti-icing performance at an altitude of 1—4 km, a maximum flight altitude of 8 km, a cruising speed of 40 m/s, and a temperature of −10——3 ℃. The developed anti-icing hybrid skin has been applied on a certain type of UAVs. The bio-inspired anti-icing skin has broad application prospects in large transport aircraft, helicopters, wind power generation, and high-speed trains.

References

[1] CAO Y, WU Z, SU Y, et al. Aircraft flight characteristics in icing conditions[J]. Progress in Aerospace Sciences, 2015,74: 62-80.

[2] CAO Y, TAN W, WU Z. Aircraft icing: An ongoing threat to aviation safety[J]. Aerospace Science and Technology, 2018,75: 353-385.

[3] FREEMAN A I, SURRIDGE B W J, MATTHEWS M, et al. Understanding and managing de-icer contamination of airport surface waters: A synthesis and future perspectives[J]. Environmental Technology & Innovation, 2015,3: 46-62.

[4] HUO Hengxi, LIU Peng, JIA Lijie. Research of the wing hot air anti-icing system for the civil aircarft[J]. Civil Aircraft Design and Research, 2010, 99(4): 16-18. (in Chinese)

[5] HE Zhoudong, ZHU Yongfeng, ZHOU Jinfeng. Study on electro-impulse de-icing technology[J]. Journal of Experiments in Fuid Mechanics, 2016, 30(2): 38-45. (in Chinese)

[6] PEI Runan, ZHU Dongyu, SHU Jun. Icing test of characteristic of runback ice accretions on horizontal tail[J]. Journal of Nanjing University of Aeronautics & Astronautics, 2022, 54(6): 1074-1082. (in Chinese)

[7] HU Linquan. Application status and technical difficults for civil aircraft wing electrothermal anti-/de-icing[J]. Aeronautical Science & Technology, 2016, 27(7): 8-11. (in Chinese)

[8] HU Mingyi. Harm of ice accumulation to aircraft and antideicng method[J]. Technology Wind, 2021, 445(5): 17-18. (in Chinese)

[9] ZHU Y, WANG Z, LIU X, et al. Anti-icing/de-icing mechanism and application progress of bio-inspired surface for aircraft[J]. Transactions of Nanjing University of Aeronautics and Astronautics, 2022, 39(5): 541-560.

[10] BARTHLOTT W, NEINHUIS C. Purity of the sacred lotus, or escape from contamination in biological surfaces[J]. Planta, 1997,202(1): 1-8.

[11] LIN Y, CHEN H, WANG G, et al. Recent progress in preparation and anti-icing applications of superhydrophobic coatings[J]. Coatings, 2018,8(6): 208.

[12] KREDER M J, ALVARENGA J, KIM P, et al. Design of anti-icing surfaces: Smooth, textured or slippery?[J]. Nature Reviews Materials, 2016, 1(1): 15003.

[13] GUO Z, LIU W. Biomimic from the superhydropho-

bic plant leaves in nature: Binary structure and unitary structure[J]. Plant Science, 2007, 172(6): 1103-1112.

[14] BHUSHAN B, HER E. Fabrication of superhydrophobic surfaces with high and low adhesion inspired from rose petal[J]. Langmuir: the ACS Journal of Gurfaces and Colloids, 2010, 26(11): 8207-8217.

[15] FENG X J, JIANG L. Design and creation of superwetting/antiwetting surfaces[J]. Advanced Materials, 2006,18(23): 3063-3078.

[16] ZHAO W, WANG L, XUE Q. Fabrication of low and high adhesion hydrophobic Au surfaces with micro/nano-biomimetic structures[J]. The Journal of Physical Chemistry C, 2010,114(26): 11509-11514.

[17] HANH V T H, TRUONG M X, NGUYEN T B. Anti-icing approach on flexible slippery microstructure thin-film[J]. Cold Regions Science and Technology, 2021,186: 103280.

[18] HE Y, JIANG C, CAO X, et al. Reducing ice adhesion by hierarchical micro-nano-pillars[J]. Applied Surface Science, 2014,305: 589-595.

[19] GE C, YUAN G, GUO C, et al. Femtosecond laser fabrication of square pillars integrated Siberian-Cocklebur-like microstructures surface for anti-icing[J]. Materials & Design, 2021,204: 109689.

[20] TANG L, WANG N, HAN Z, et al. Robust superhydrophobic surface with wrinkle-like structures on AZ31 alloy that repels viscous oil and investigations of the anti-icing property[J]. Colloids and Surfaces A: Physicochemical and Engineering Aspects, 2020, 594: 124655.

[21] WANG D, SUN Q, HOKKANEN M J, et al. Design of robust superhydrophobic surfaces[J]. Nature, 2020,582(7810): 55-59.

[22] BORREBÆK P O A, JELLE B P, ZHANG Z. Avoiding snow and ice accretion on building integrated photovoltaics-challenges, strategies, and opportunities[J]. Solar Energy Materials and Solar Cells, 2020, 206: 110306.

[23] ANDREWS R W, POLLARD A, PEARCE J M. A new method to determine the effects of hydrodynamic surface coatings on the snow shedding effectiveness of solar photovoltaic modules[J]. Solar Energy Materials and Solar Cells, 2013,113: 71-78.

[24] Cvil Aviation Administration of China. Airworthiness standards for transport category aircraft[S]. Beijing: Cvil Aviation Administration of China, 2011: 186-189.(in Chinese)

Acknowledgements This work was supported in part by the National Natural Science Foundation of China (Nos. 51875478, 51735011, 52111530127) and the Foundation of National Key Laboratory of Science and Technology on Aerodynamic Design and Research (No.61422010102). The authors realize that the time and space available for a review of such an ambitious subject are limited and, thus, regretfully, we are unable to cover many important contributions.

Authors Ms. **YAN Zexiang** received the B.S. degree in micro-electro-mechanical system from Northwestern Polytechnical University in 2019. Her research is focused on micro- and nano-structure for anti-icing surface and relevant fields.

Prof. **HE Yang** received the B.S., M.S., and Ph.D. degrees in mechanical engineering from Northwestern Polytechnical University in 2002, 2005, and 2011, respectively. He has presided over projects such as the National Natural Science Foundation of China, the Civil Aircraft Special project. He has won first prize of Shaanxi Science and Technology Award, first prizes of China Machinery Industry Science and Technology Award. He is currently mainly engaged in the research of bionic micro-nano structures for aircraft anti-icing and drag reduction technology.

Prof. **YUAN Weizheng** received the B.S. degree and M.S. degree in 1982 and 1986, respectively. He started the research in the field of MEMS in 1992 when he was studying in France and received the Ph.D. degree in 1996. He is the director of the Key Laboratory of Aerospace Micro-nano Systems of the Ministry of Education and the person in charge of the construction of the World-Class Discipline of Mechanical Engineering in Northwestern Polytechnical University. He was the distinguished professor in 2006, President of the 25th World Summit of Micro-machine in 2019. He is also an executive director of the Chinese Society of Mechanical Engineering, an executive director of the Chinese Society of Micro and Nanotechnology, and an editorial member of the Journal of Mechanical Engineering.

Author contributions Ms. **YAN Zexiang** contributed to the design and preparation of the material and wrote the manuscript. Prof. **HE Yang** conducted the analysis and experiments. Prof. **YUAN Weizheng** contributed to the discussion and application of this study. All authors commented on the manuscript draft and approved the submission.

Competing interests The authors declare no competing interests.

(Production Editor: XU Chengting)

仿秦岭箭竹叶微纳结构疏冰蒙皮

燕则翔[1,2], 何 洋[1,2], 苑伟政[1,2]

(1. 西北工业大学空天微纳系统教育部重点实验室, 西安 710072, 中国;
2. 西北工业大学陕西省微/纳米系统重点实验室, 西安 710072, 中国)

摘要: 飞机结冰极大威胁飞行安全,严重时导致机毁人亡。适应恶劣寒冷环境的飞机防除冰技术是国际难题,也是中国多型飞机研制必须突破的重大技术瓶颈。本文首次提出一种仿生疏冰雪对象——秦岭箭竹,建立仿秦岭箭竹叶多层不等高微纳结构,揭示了这种独特结构对过冷微小水滴形成弹跳,滚动成冰及滑落的疏冰机制;提出一种基于分层组装的柔性大幅面微纳结构制备方法,实现仿秦岭箭竹叶疏冰结构制备;获得的仿秦岭箭竹叶疏冰表面相较于同材料光滑表面冰粘附强度降低80%,表明秦岭箭竹叶微纳结构具有优异的疏冰效果。结合实际工程应用,研制基于功率密度分区的仿生与电热相结合的疏冰复合蒙皮,据此获得的疏冰复合蒙皮成功完成中小型无人机防除冰功能飞行,并且已成功列装某型号高原型无人机,满足了高寒条件下的有效防除冰飞行要求。仿秦岭箭竹叶疏冰蒙皮也在大型运输机、直升机,以及风力发电、高速列车等领域具有广阔的应用前景。

关键词: 飞机结冰;仿生表面;微纳结构;飞机蒙皮